water

MDPI

Article

Evaluation of Kinetic, Equilibrium and Thermodynamics of Cationic Ion Using Agro-Industrial Residues of Plantain (*Musa paradisiaca*)

Angel Villabona-Ortíz [1], Ángel Darío González-Delgado [2,*] and Candelaria Tejada-Tovar [1,*]

[1] Process Design and Biomass Utilization Research Group (IDAB), Chemical Engineering Department, Universidad de Cartagena, Avenida del Consulado St. 30, Cartagena de Indias 130015, Colombia; avillabonao@unicartagena.edu.co

[2] Nanomaterials and Computer Aided Process Engineering Research Group (NIPAC), Chemical Engineering Department, Universidad de Cartagena, Avenida del Consulado St. 30, Cartagena de Indias 130015, Colombia

* Correspondence: agonzalezd1@unicartagena.edu.co (Á.D.G.-D.); ctejadat@unicartagena.edu.co (C.T.-T.)

Abstract: This study aimed to evaluate the adsorptive capacity of Cr (VI) on the residues of the plantain starch extraction process in a batch system, determining the effect of temperature, initial concentration and adsorbent dose. The adsorbent was characterized by FTIR and SEM. The Cr (VI) solution was placed in contact with the adsorbent at pH 2 and 200 rpm. The results revealed the presence of COO^-, OH^- and CH_x^+ functional groups in the adsorbent. In addition, the adsorption process is controlled by chemisorption and electrostatic interactions. We also found that temperature and adsorbent dose are the variables with significant influence. The highest adsorption capacity was 64.46 mg/g at 55 °C, 200 mg/L and 0.14 g of biomaterial. Based on the kinetic behavior, it was found that the data are adjusted by the pseudo-second order, Elovich and intraparticle diffusion models. The fit of the isotherms to the Freundlich and Dubinin–Radushkevich models establishes that the limiting step of the process is the chemical reaction. The thermodynamic parameters determine that the process is endothermic, with strong biomass–metal bonds that are favorable and spontaneous as the temperature increases. The results indicate that the residual plantain pulp is a residue that can be used in the removal of Cr (VI) ions, and it contributes to the state of the art in terms of the use of new agro-industrial waste.

Keywords: bioadsorption; chromium (VI); isothermal study; kinetic modeling

Citation: Villabona-Ortíz, A.; González-Delgado, Á.D.; Tejada-Tovar, C. Evaluation of Kinetic, Equilibrium and Thermodynamics of Cationic Ion Using Agro-Industrial Residues of Plantain (*Musa paradisiaca*). *Water* **2022**, *14*, 1383. https://doi.org/10.3390/w14091383

Academic Editors: Tushar Kanti Sen and Yanbo Zhou

Received: 29 December 2021
Accepted: 19 April 2022
Published: 24 April 2022

1. Introduction

The effects on ecosystems and public health caused by contamination by heavy metals such as chrome, lead, mercury, cadmium, and copper, among others, are a problem of global concern; this is because they resist biodegradation processes due to their chemical stability, easy migration in the environment and their tendency to bioaccumulate [1]. Cr (VI) enters the water sources in effluents from different industrial sectors such as fertilizer manufacturing, batteries, electroplating, paints, photography, tanneries, and electronic materials, among others [2]. In contact with water, chromium is found in the oxidation states +3 and +6, the latter being the most worrying one because it diffuses easily in the environment and penetrates the biological barriers [3], having carcinogenic and mutagenic effects. In the pH range 2–6, the predominant form is $Cr_2O_7^{2-}$ and $HCrO_4^-$, at pH greater than or close to 6, chromium is present in the form of CrO_4^{2-} ions, and the affinity of this anion is very low compared to $Cr_2O_7^{2-}$ and $HCrO_4^-$. So, at lower pH, the bioadsorbent surface is highly protonated due to H^+ ions; therefore, there is a strong electrostatic attraction between the positively charged surface and $Cr_2O_7^{2-}$ and $HCrO_4^-$, and it is 500 times more toxic than Cr (III) [4].

Consequently, multiple technologies have been implemented for the removal of this metal present in water, due to its high resistance to degradation, such as ion exchange, filtration, electrochemical treatment, oxidation, catalytic oxidation, precipitation, evaporation, and bioremediation, among others [5]. However, the high energy consumption, operating costs, sludge accumulation and large amounts of input chemicals make these methods very expensive in general [6]. Thus, bioadsorption is an alternative to the processes mentioned above due to the great efficiency obtained by the agro-industrial waste due to its lignocellulosic origin [7], allowing the recovery of the metal and reuse of the bioadsorbent [3]. Several studies have reported on the use of reject products in the removal of Cr (VI) such as rice husks [4] and nut [8], coffee pulp [9] and corn waste [10], evaluating parameters such as pH, adsorbent dose, initial concentration, contact time and temperature on the adsorption capacity of the biomaterials; it was found that these are good adsorbents of Cr (VI) present in solution due to its high content of lignocellulosic compounds by the presence of active groups of adsorption as hydroxyl, carboxyl, alcohols, amines and hydrocarbons [8].

On the other hand, approximately 102 million plantains are produced annually in the world, where 35% of each fruit produces approximately 36 million tons of waste [11]. In Colombia, the large number of plantain crops (*Musa paradisiaca*), specifically in the department of Bolivar, has generated an increase in post-harvest waste, because their production is focused on marketing or as a household food option, representing 10% of the total plantain crop produced. For this reason, this research proposes the use of residual pulp from the process of obtaining plantain starch as a bioadsorbent of Cr (VI) in solution; this is because plantain starch is a food alternative, for the use of large quantities of harvested plantains, and taking into account the wide use of starch (textile industry, paper, bioplastics and rubber manufacturing) [8]. The use of waste from starch production as an adsorbent is an interesting alternative due to the large volumes generated after the process of obtaining starch, considering that it has a yield of 20% [12]; considering that starch is used in different sectors of industry, especially in the food industry, the textile, paper, bioplastic, dextrin and glue industries. Currently, there is a trend toward the search for new alternatives of native starches or physically or chemically modified starches [13]. In previous investigations to the present work, this plantain starch pulp was satisfactorily employed in the removal of chromium (VI) in packed bed system, reaching an adsorption capacity for the column of 29.85 mg/g, and the temperature and the height of the bed having a significant effect on the process [14].

That is why the objective of the present project was to optimize the effect of the initial concentration of contaminant, temperature and dose of adsorbent by means of the Response Surface Methodology (RSM), using residues from obtaining banana starch in the removal of chromium (VI). The adsorption mechanism was evaluated by fitting the experimental kinetic data to the pseudo-first-order, pseudo-second order and Elovich models. Adsorption equilibrium was studied by fitting the data to the Langmuir, Freundlich and Dubinin–Radushkevich models. The change in Gibbs' free energy (ΔG°), enthalpy (ΔH°) and entropy (ΔS°) was estimated to establish spontaneity, favorability and the influence of temperature on the process. This basic study will serve as a support for the future scaling up of the process in question.

2. Materials and Methods

Merck Millipore brand analytical grade sodium dichromate ($Na_2Cr_2O_7$) was used to prepare the synthetic solution contaminated with Cr (VI), NaOH and HCl 1 N to adjust the pH. Batch adsorption tests were performed in an orbital shaker brand Lab Shaker Incubator model IN-666 with temperature control. All experimental assays will be developed at pH 2 and 200 rpm.

2.1. Preparation of the Biomass

The plantain (*Musa Paradisiaca*) was collected as post-harvest waste in a rural area of the Bolivar department. The residual plantain pulp was obtained as a rejection product of

the starch extraction process; for this, the raw material was peeled, washed with distilled water, and submerged in a 0.25% NaOH solution at 5 °C for 18 h. Then, the residue of interest was separated from the starch by filtration [15,16], was dried at 40 °C in an oven to a constant mass, reduced in size in a roller mill, and size graded in a shaker-type sieve shaker selecting a particle of 0.5 for experiments. The residual plantain pulp was characterized by FTIR analysis before and after the Cr (VI) adsorption process to determine the intervening functional groups, for which a Nicolet 8700 spectrophotometer was used, making 128 sweeps in the range of 400–4000 cm^{-1}. Scanning Electron Microscopy (SEM) and X-Ray Spectroscopy (EDS) were also performed using a JEOL model JSM 6490-LV scanning electron microscope with acetylene/air flame to study the surface of the bioadosbent and the adsorption mechanisms.

2.2. Adsorption Tests

The experimental development of the present research was carried out following a design of continuous linear factor experiments on central composite design with response surface, designed with Statgraphics Centurion XVI.II® (Table 1), for a total of 16 experiments. These levels were chosen for the variables taking as a starting point values evaluated in previous studies and with this design to carry out a more complete study.

Table 1. Experimental ranges and levels of variables for adsorption assays.

Independent Variables	Unit	Range and Level				
		Lower Value	Low Value	Center Point	High Value	Higher Value
Temperature	°C	29.80	40	55	70	80
Adsorbent amount	g	0.14	0.36	0.68	1.00	1.20
Initial concentration	mg/L	31.80	100	200	300	368.20

A 1000 mg/L Cr (VI) stock solution was used, for which 2828 g $K_2Cr_2O_7$ was added in 1 L of deionized water, from which it was diluted to obtain the concentrations established in the design of the experiments. Adsorption tests were performed individually in a shaker by placing 100 mL of solution in contact with the adsorbent with 200 rpm agitation and pH 2 for 24 h [17]. The remaining metal concentration in the solution was made following the ASTM for the determination of chromium in water D1867, which is a method that uses the colorimetric method of 1,5-Diphenylcarbazide at 540 nm in a UV-Vis spectrophotometer model BK-UV 1900 [10]. The removal performance and adsorption capacity of the adsorbent were determined by Equations (1) and (2):

$$RE(\%) = \frac{C_i - C_f}{C_i} \times 100 \quad (1)$$

$$q_t = \frac{(C_i - C_f) \times V}{m} \quad (2)$$

where C_i and C_f are the initial and final contaminant concentrations in mg/L, V is the volume of solution in L, m is the adsorbent dose in g, q_t is the adsorbent adsorption capacity in mg/g and RE is the removal efficiency in percentage.

The statistical analysis of the experimental data was carried out with the Statgraphics Centurion XVI.II® software, which allows determining the effect of each one of the variables upon the adsorption capacity of the material by means of the analysis of variance, Pareto diagram, estimated response surface and optimization of such response that allows to maximize the adsorption capacity. From this statistical analysis and experimental results, the best conditions will be selected to develop the kinetic and equilibrium study.

2.3. Adsorption Kinetics

Adsorption kinetics was performed to establish the saturation time of the material as well as the possible interaction mechanisms that control the process. For this purpose, under the best conditions of temperature, dose of adsorbent and initial concentration, established during the adsorption tests considering the experimental design (Table 1), 10 mL of Cr (VI) solution was placed in contact and measurements of the concentration were developed at time intervals: 5, 10, 15, 20, 30, 60, 90, 180, 240, 320 and 380 min. The adjustment of the kinetic data describing the rate at which the contaminant is removed from the treated effluent was completed by the non-linearized pseudo-first order, pseudo-second order, Elovich and intraparticle diffusion kinetic models using the software OriginPro8®, and the results are presented in Table 2.

Table 2. Non-linear kinetic models.

Model	Parameter	Equation	
Pseudo-first order	q_e (mg g^{-1}): adsorption capacity at equilibrium q_t (mg g^{-1}): adsorption capacity at time t k_1 (min^{-1}): the pseudo first order constant	$q_t = q_e\left(1 - e^{-k_1 t}\right)$	(3)
Pseudo-second model	k_2 (g^{-1} min^{-1}): second order adsorption constant t (min): time	$q_t = \frac{t}{\frac{1}{k_2 q_e^2} + \frac{t}{q_e}}$	(4)
Elovich	α (mg g^{-1} min^{-1}): the initial adsorption rate of the model β (g mg^{-1}): is the constant related to the surface coverage scope and activation energy in chemisorption	$q_t = \frac{1}{\beta}\ln(\alpha\beta) + \frac{1}{\beta}\ln(t)$	(5)
Intraparticle diffusion	k_3 (mg g^{-1} $min^{-1/2}$): intraparticle diffusion constant.	$q_t = k_3 t^{\frac{1}{2}}$	(6)

2.4. Adsorption Equilibrium

Adsorption isotherms were performed by varying the initial concentration of contaminant by 25, 50, 100, 200 and 300 mg/L to determine its influence on the process when it has reached equilibrium. The experimental data were adjusted to the non-linearized Langmuir and Freundlich equations. The Langmuir model states that adsorption occurs at specific homogeneous sites within the adsorbent, assuming that all active adsorption sites are energetically identical and that the process occurs in a monolayer. The non-linear adjustment of the mathematical models was performed in software OriginPro 8®. The models are presented in Table 3 [17].

Table 3. Non-linear isotherm models.

Model	Parameter	Equation	
Langmuir	q_e (mg g^{-1}): amount of contaminant adsorbed on the bioadsorbent surface b (L mg^{-1}): ratio of adsorption/desorption q_{max} (mg g^{-1}): maximum adsorption corresponding to the saturation sites C_e (min L^{-1}): the pseudo-first order constant	$q_e = q_{max} \times \frac{bC_e}{1+bC_e}$	(7)
Freundlich	K_F (mg L g^{-2}): Freundlich constant n: adsorption intensity	$q_e = K_f C_e^{\frac{1}{n}}$	(8)
Dubinin–Radushkevich	ε: potential of Polanyi based on temperature	$q_e = q_{DR} \times e^{-K_{DR}\varepsilon^2}$	(9)
	K_{DR} (mol^2 kJ^{-2}): is the constant of Dubinin–Radushkevich related to adsorption energy E (kJ mol^{-1}): average adsorption energy per molecule of adsorbate required to transfer one mol of ion from solution to the surface of the adsorbent	$\varepsilon = RT \times \ln\left(1 + \frac{1}{C_e}\right)$	(10)
		$E = \frac{1}{\sqrt{2K_{DR}}}$	(11)

2.5. Thermodynamic Parameters

The thermodynamic study of adsorption allows establishing possible mechanisms of adsorption (endothermic/exothermic, favorability and spontaneity of the process); it is performed by calculating the change in Gibbs' standard free energy ($\Delta G°$), standard enthalpy ($\Delta H°$), and standard entropy ($\Delta S°$), which were determined according to Equations (12)–(14) [18].

$$K_c = \frac{q_e}{C_e} \tag{12}$$

$$\Delta G = -RT \times \ln K_c \tag{13}$$

$$\ln K_c = \frac{-\Delta H}{RT} + \frac{\Delta S}{R} \tag{14}$$

where K_c is the equilibrium constant in mg g^{-1}, q_e is the equilibrium solid phase concentration (mg g^{-1}), and C_e is the equilibrium concentration (mg L^{-1}), R is the ideal gas constant 8314 J $mol^{-1}K^{-1}$, T is the absolute temperature in K, $\Delta H°$ and entropy $\Delta S°$ are determined from the slope and y-axis intercept of the Arrhenius graph of lnKc vs. T^{-1}, respectively.

3. Results

3.1. Characterization of the Bioadsorbent

The FTIR spectra in Figure 1 correspond to the residual plantain pulp before and after the removal of Cr (VI). Before the adsorption, the peaks between 3000 and 3500 cm^{-1} attributed to the presence of =CH- (alkenes and aromatics) are highlighted, between 3200 and 3500 cm^{-1}, characteristic signs of the vibration stretching of OH appear. The peak at 2927.94 cm^{-1} is due to vibrations of the CH groups; between 2000 and 2500 cm^{-1}, there are carboxylic acid signs that may be due to the stretching of OH.

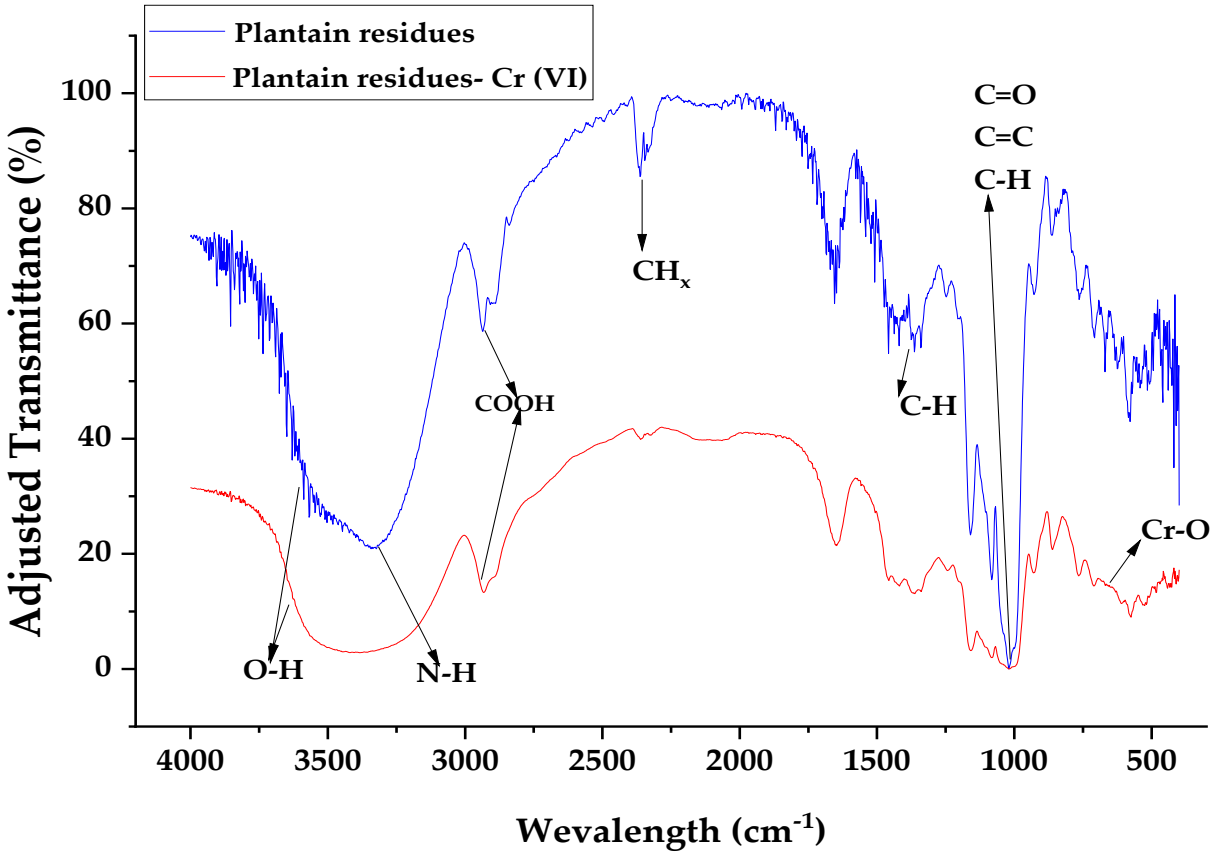

Figure 1. Normalized IR spectrum of plantain residues before (blue) and after (red) Cr (VI) adsorption.

On the other hand, between 1000 and 1200 cm^{-1}, there is the presence of alcohols due to the stretching vibrations of the C-OH bond [1]. After the adsorption process, an increase in the width of the spectral bands and a slight decrease in intensity can be observed. The decrease provided by the variation of the adsorption frequency can be attributed to the binding of Cr (VI) ions to the different functional groups corroborated in the peak at 2341 cm^{-1} due to a possible interaction of hydrogen bridges as well as in the change of intensity of the absorption peak at 2927.94 cm^{-1} attributed to the vibrations of the methyl, methylene and methoxy groups present in the biomass that facilitate the adsorption [19].

Figure 2 shows the SEM microphotographs and the EDS spectrum of the banana starch residues before and after adsorption of Cr (VI). It can be seen that the bioadsorbent exhibits a uniform and cylindrical surface, without micropores according to the surface area of 3859 m^2/g, pore size of 486 nm and pore volume of 4×10^{-7} m^3 kg^{-1} [20]. This structure could be due to the use of NaOH during the preparation of the bioadsorbent, which can cause changes in the material, increasing its adsorption capacity [21]. After adsorption, Cr (VI) is observed in the high-intensity peaks at 0.6, 5.6 and 6 keV; the increase in C; the decrease in O, K; and the disappearance of Na in 1 ekV and K in 3.4 keV, which could be due to the formation of links between the ion and the active centers of the bioadsorbent [1]. Furthermore, the formation of white precipitates on the material and the smoothing of the cylindrical surface is observed, so it is determined that the mechanism of ion adsorption in biomaterials is given by ion exchange between the metals under study and the active centers of the material [22]. Thus, micro-precipitations and complexes are formed when Cr (VI) is captured in the active centers [23].

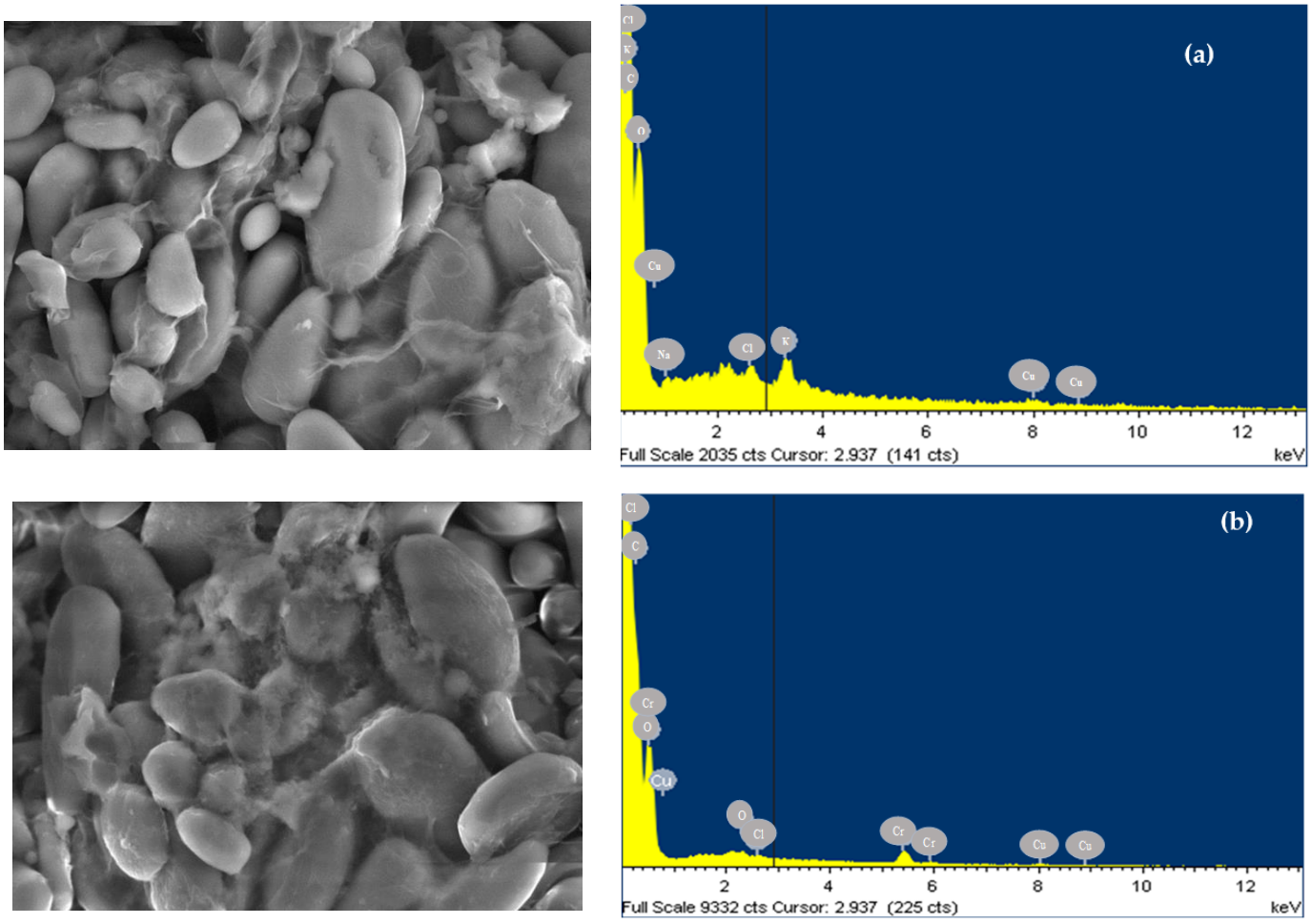

Figure 2. SEM micrographs amplified ×1000 and EDS spectrum of banana starch residues (**a**) before and (**b**) after Cr (VI) adsorption.

3.2. Adsorption Test and Statistical Analysis

After carrying out the Cr (VI) adsorption tests using the residual plantain cake, the effect of the amount of biomass, the temperature and the initial metal concentration was evaluated by calculating the adsorption capacity of Cr (VI). In Table 4, the results of adsorption capacity at each of the conditions studied are shown. It is established experimentally that it is at 55 °C, 200 mg/L and 0.135 g of biomaterial where a higher adsorption capacity of 64.46 mg/is obtained.

Table 4. Adsorption capacity of Cr (VI) on residual plantain pulp at different conditions of temperature, adsorbent dose and initial concentration.

Adsorbent Dose (g)	Temperature(°C)	C_i (mg/L)	C_f (mg/L)	ER (%)	q_t (mg/g)
1.00	70	100	95.08	4.92	0.492
0.68	55	31.82	18.33	10.95	1.99
0.68	80.2	200	0.64	99.18	29.43
0.68	29.8	200	97.37	51. 31	15.15
0.36	70	100	3.30	96.70	27.24
1.00	40	300	216.72	27.76	8.33
0.68	55	368.2	95.08	74.17	40.31
0.68	55	200	151.90	24.05	7.099
0.36	70	300	230.96	69.36	19.45
0.68	55	200	175.95	24.05	3.55
0.36	40	300	286.86	13.14	3.70
1.22	55	200	131.72	68.29	5.59
1.00	70	300	230.17	69.83	6.98
0.36	40	100	40.68	59.32	16.71
1.00	40	100	0.51	99.49	9.95
0.14	55	200	112.90	87.10	64.46

The increase in temperature had a positive effect on the adsorption (Figure 3); this may be due to a higher rate of diffusion of the ions in the pores of the bioadsorbent by the formation of bonds with the functional groups improving intraparticle diffusion [24]. This behavior coincides with that reported by Chinyelu Ijeamaka et al. [25] and Villabona-Ortíz et al. [17], who found that an increase in temperature between 50 and 90 °C benefits the process of removing Cr (VI) on coconut shells; this is due to the endothermic nature of the process and the increased kinetic speed of adsorption.

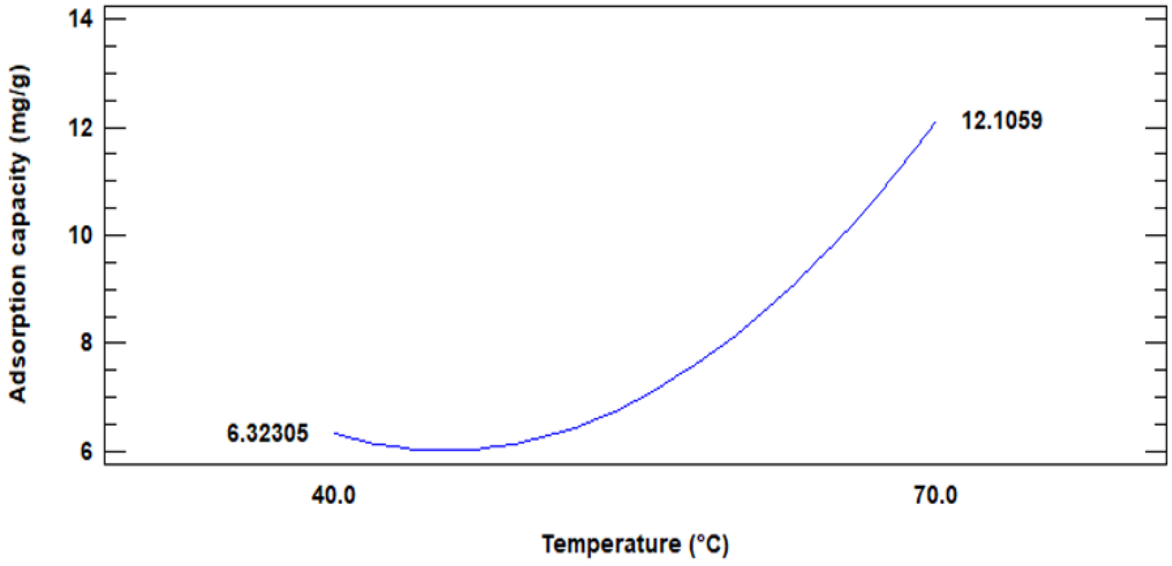

Figure 3. Main effect plot of temperature on the adsorption capacity of Cr (VI).

Figure 4 shows the effect of the adsorbent dose on the removal of Cr (VI). It is observed that the adsorption capacity of the metal decreases as the amount of adsorbent increases; the maximum capacity and percentage of adsorption was reached at the lowest evaluated dose of adsorbent. This is attributed to the increase in active sites available for adsorption; when adding a higher amount of material, there will be a large number of active sites available, which will not be saturated at the end of the process. In addition, there may be competition from solute ions for limited available binding sites, electrostatic interactions, overlapping or aggregation of adsorption sites, low surface area, interference between binding sites, and contact of ions below higher densities of adsorbents [5].

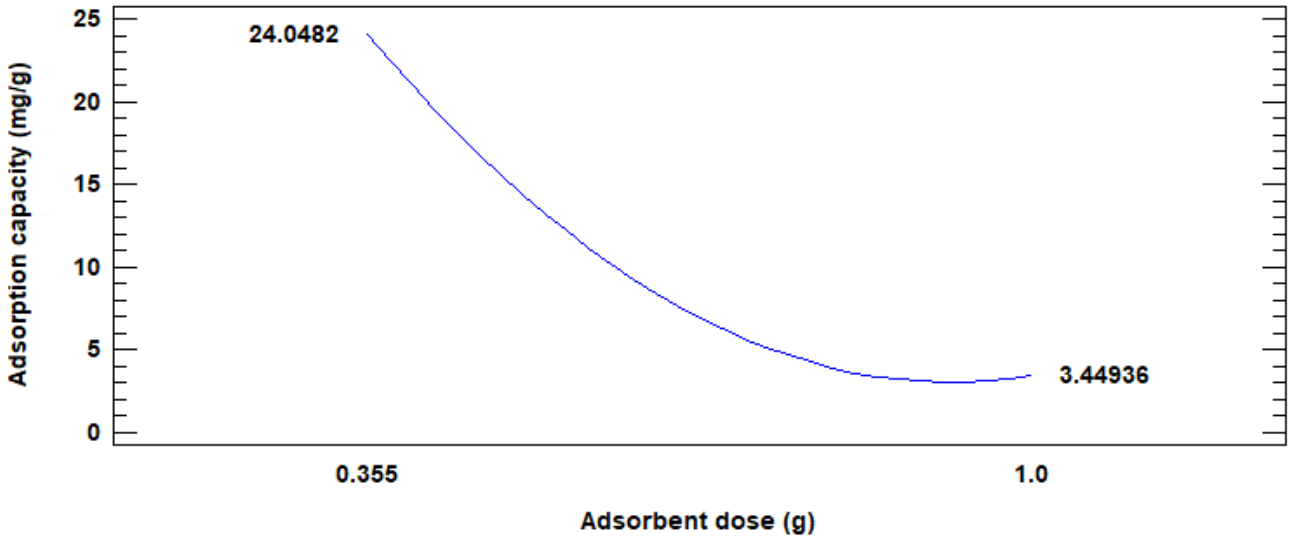

Figure 4. Main effect plot of the adsorbent dose on the adsorption capacity of Cr (VI).

A wide range of initial Cr(VI) concentrations were selected from 31.82 to 368 mg/L for determining its main effect on the adsorption capacity of Cr(VI) onto plantain starch residues; the results are shown in Figure 5. An increase in the adsorption capacity is observed with increasing initial concentration, which can be attributed to the increase in the adsorption driving force due to the availability of contaminant when the surface of the bioadsorbent is unsaturated [26]. This behavior was evidenced in the use of orange peels [27], oak acorn [28] and *Phanera vahlii* [29]; and it can be explained due to the exhaustion of the Cr (VI) ions at low concentration, since almost all Cr (VI) ions have been adsorbed on the surface and removed by the reducing elements of the biosorbent.

Table 5 shows the results obtained from the analysis of variance (ANOVA), which was performed with the Statgraphics Centurion XVI.I software; it is observed that the most relevant factors in the design are the dose of adsorbent and temperature, since the *p*-value less than 0.05 indicates this. It is observed that the effects with statistical significance on the process are the temperature and dose of adsorbent; this can be explained since these variables are determinants on the rate of diffusion from the solution to the active sites available on the surface and the pores of the adsorbent [29].

Equation (15) describes the behavior of the experimental data of Cr (VI) adsorption onto plantain residues.

$$q_t = 58.18 - 0.22 \times T - 80.03 \times M - 0.15 \times C + 0.008 \times T^2 - 0.96 \times T \times M + 0.001 \times T \times C + 59.76M^2 + 0.1M \times C + 0.0001 \times C^2 \quad (15)$$

where q_t is the adsorption capacity, T is the temperature, M is the adsorbent dose, and C is the Cr(VI) initial concentration. The positive and negative signs before the terms indicate the synergistic and antagonistic effect of the respective variables [30].

The predictions provided by the RSM for Cr (VI) are shown in the function graph as an estimated area (Figure 6). From the values estimated in the response surface to have a

high efficiency in the adsorption of Cr (VI) ions, the analysis indicated the optimal values to maximize the removal with the minimum possible energy consumption in the batch system, establishing a concentration initial of 200 mg/L, temperature of 55 °C and adsorbent dose of 0.14 g.

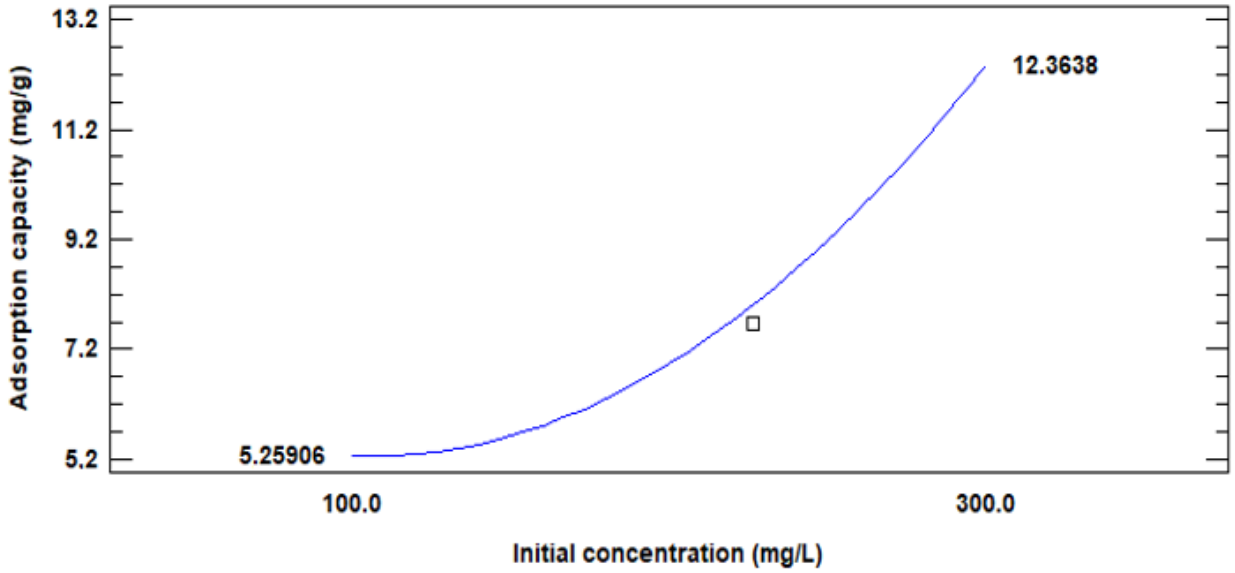

Figure 5. Main effect plot of the initial concentration on the adsorption capacity of Cr (VI).

Table 5. Analysis of variance of Cr (VI) adsorption.

Source	Sum of Squares	Ratio-F	*p*-Value
A: Temperature	158.25	0.48	0.04
B: Adsorbent dose	1302.18	3.95	0.03
C: Initial concentration	126.19	0.38	0.56
AA	58.77	0.18	0.69
AB	113.16	0.34	0.58
AC	5.01	0.02	0.91
BB	456.69	1.39	0.28
BC	43.56	0.13	0.73
CC	41.47	0.13	0.74
Total error	1976.93		
Total (corr.)	4190.36		

3.3. Cr (VI) Adsorption Kinetics

Figure 7 shows the fit of Cr (VI) adsorption kinetics data on plantain residual pulp to the pseudo-first order, pseudo-second order, Elovich and intraparticle diffusion models at the best experimental conditions found (55 °C, 200 mg L^{-1} and 0.1 g of adsorbent).

It was found that the saturation time of the material at 60 min and the equilibrium was reached at 100 min, indicating the reduction in the active sites of the biomass that have been occupied by Cr (VI) [31]. From the values of the adjustment parameters shown in Table 6, it is established that the models evaluated adjust the metal removal kinetics, being the q_e determined by the pseudo-second order model the one that is closer to the experimental value, so it can be said that the model is controlled by the chemical reaction that occurs during the ion exchange of the active centers of the material and the metal, obeying a second-order reaction law [32]. The fit of the adsorption kinetics of Cr (VI) to the intraparticle diffusion model suggests that the adsorption occurs initially by diffusion of the metal through the solution to the outer surface of the adsorbent, which would imply the rapid rate of adsorption during the first minutes [33]; after this rapid adsorption, the

diffusion of the metal through the pores of the adsorbent would occur, the process was controlled by the phenomenon of diffusion and chemical adsorption [2].

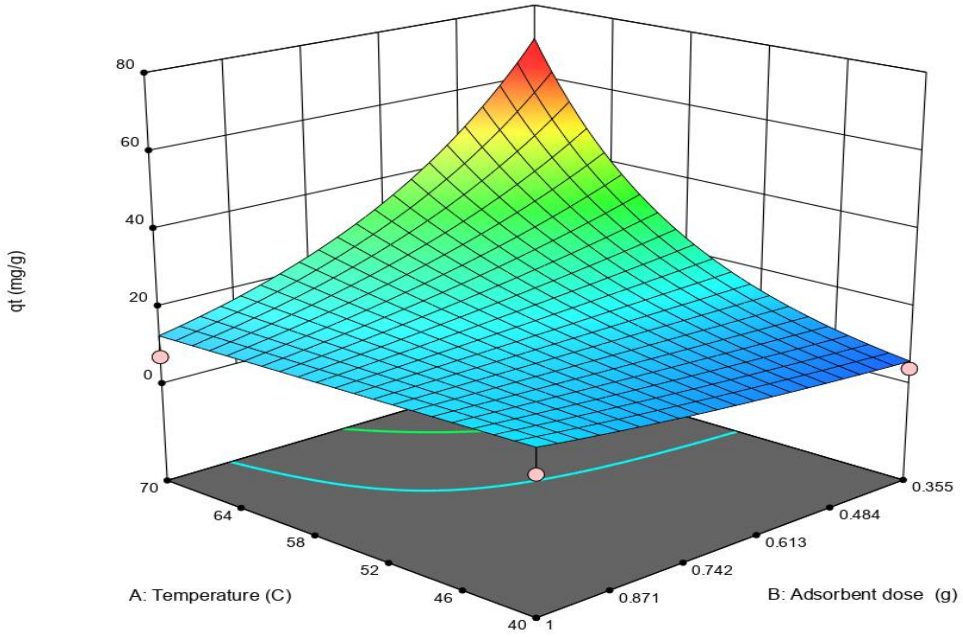

Figure 6. Estimated Response Surface for chromium (VI) adsorption capacity with relevant data points in pink.

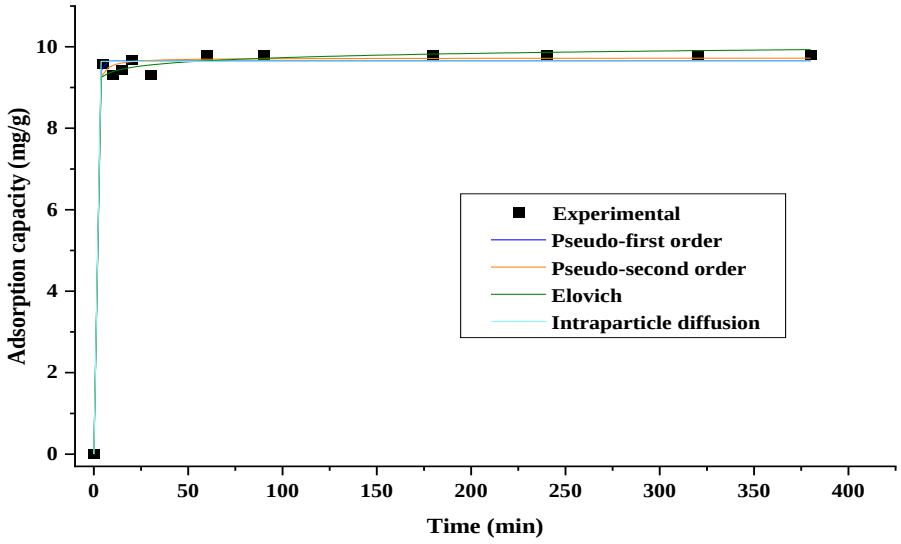

Figure 7. Non-linear adjustment of the adsorption kinetics of Cr (VI) at pH 2, 55 °C, 200 mg L^{-1} and 0.14 g of adsorbent.

From Figure 8, it can be said that linear forms of Elovich and intraparticle diffusion models do not have a good fitting of linearized experimental data. Thus, it could be explained by the fast adsorption in the initial stages of the process, which was enhanced by the free active centers and the availability of metal in the solution. In addition, it was found that linearized pseudo-first and pseudo-second order models describe the process, which coincide with the findings when using non-linear models. Nevertheless, after the good adjusting of a linearized form of pseudo-first and pseud-second order models, the determined q_e is nearest to experimental data when the modeling is made with non-linearized models [34].

Table 6. Modeling adjustment parameters of Cr (VI) adsorption kinetics.

Model	Parameter	Non-Linear	Linear
Pseudo-first order	q_e	9.65	9.34
	k_1	4.92	0.08
	R^2	0.99	0.99
	SS	9.19	0.16
Pseudo-second order	k_2	2.99	0.24
	q_e	9.73	9.81
	R^2	0.99	0.99
	SS	8.19	0.02
Elovich	β	1.20×10^{40}	10.56
	α	10.243	9.79
	R^2	0.997	0.53
	SS	6.92	0.19
Intraparticle diffusion	k_3	9.644	0.02
	C		9.43
	R^2	0.995	0.51
	SS	7.0435	0.20

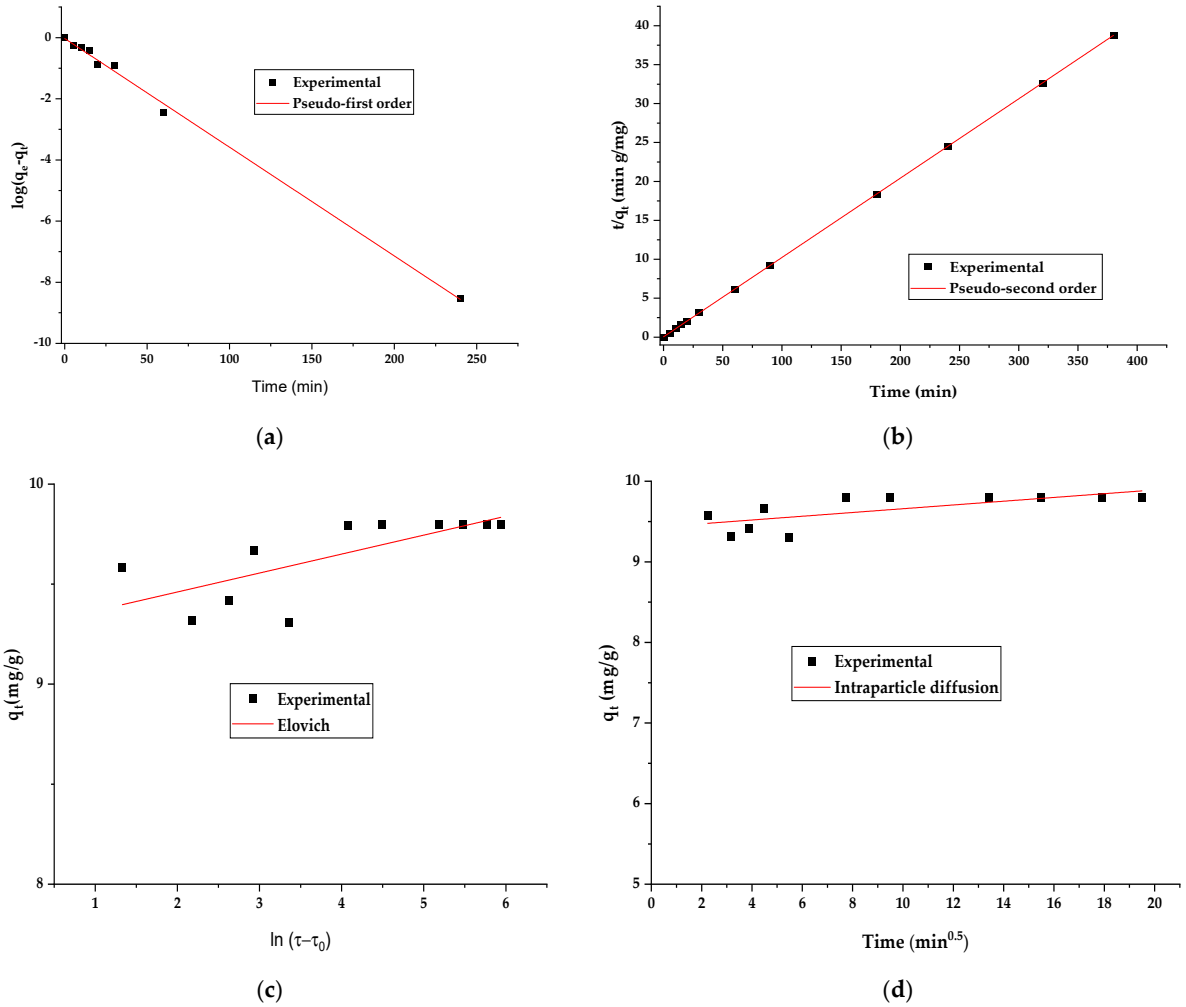

Figure 8. Kinetic linear adjustment of the adsorption kinetics of Cr (VI) to (**a**) pseudo-first order model, (**b**) pseudo-second order mode, (**c**) Elovich and (**d**) intraparticle diffusion; at pH 2, 55 °C, 200 mg L^{-1} and 0.14 g of adsorbent.

3.4. Adsorption Equilibrium

The initial concentration of the metal was varied at intervals of 25, 50, 100, 200 and 300 mg/L, keeping the temperature and dose of adsorbent at the best conditions found, in order to understand the interaction forces that control the process [35]. Figure 9 shows the fit of the experimental equilibrium data to the Langmuir, Freundlich and Dubinin–Radushkevich isothermal models; the fitting parameters are shown in Table 7.

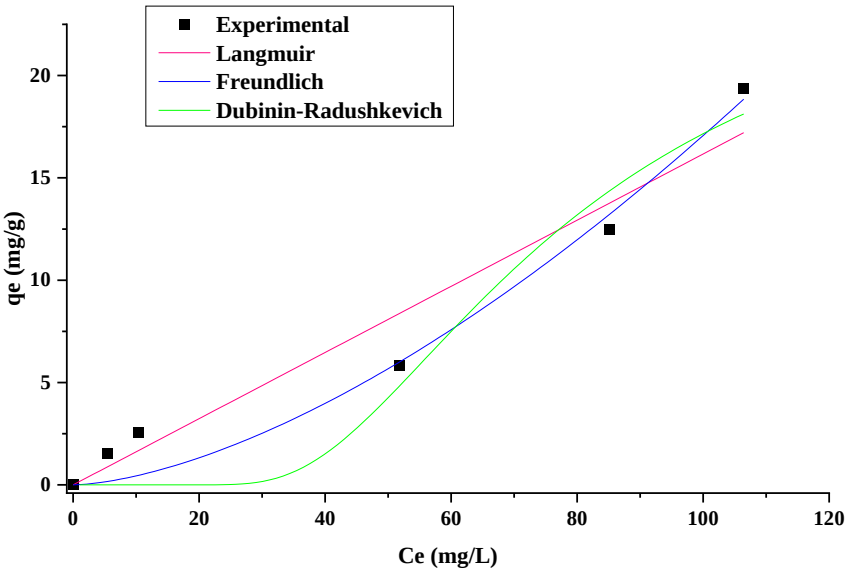

Figure 9. Non-linear modeling of the Cr (VI) adsorption isotherm at pH = 2, 55 °C and 0.14 g of adsorbent.

Table 7. Modeling adjustment parameters of the Cr (VI) adsorption isotherm at pH = 2, 55 °C and 0.14 g of adsorbent.

Isotherm Model	Parameters	Non-Linear	Linear
Langmuir	q_{max}	44.02	40.00
	b	3.67×10^{-6}	5.62×10^{-4}
	R^2	0.94	0.26
Freundlich	K_f	0.01	0.40
	$1/n$	1.89	1.30
	n	0.63	0.77
	q_F	10.10	7.94
	R^2	0.97	0.95
Dubinin–Radushkevich	q_{DR}	27.46	9.64
	K_{DR}	6.39×10^{-9}	1.30×10^{-4}
	E	8.85	61.89
	R^2	0.93	0.70

The results show that Freundlich's and Dubinin–Radushkevich's models best fit the data. The adjusting to Freundlich's model suggests that adsorption occurs by multilayers at the bioadsorbent surface with no uniform adsorption affinities between the active centers and pollutant. On the other hand, the description of equilibrium data by the equation of Dubinin–Radushkevich means that the mechanism controlling the process is the chemical reaction and that adsorption takes place preferably inside the pores of the material [36]. From the value of parameter E of Dubinin–Radushkevich's model, it can be said that the process is controlled by chemisorption with strong interactions between the metal and the active adsorption centers, as this is greater than 8 kJ mol^{-1} [25]; adjustment to this

model assumes that the bioadsorbents under study have a heterogeneous structure, which is required by the Dubinin–Radushkevich isotherm [37].

From the adjustment of data to the linearized models shown in Figure 10, it was found to have a good description only by the linearized Freundlich model. The calculated maximum adsorption capacity of starch residues for Cr (VI) adsorption using the non-linear Freundlich isotherm was greater than the corresponding values while using the linear form, respectively, by a factor of 1.8. In addition, comparing the maximum adsorption capacity (q_F) produced by application of the Freundlich and Langmuir models reveals that predicted q_F using the Freundlich isotherm is markedly lower than the corresponding values obtained by the Langmuir expression. Low values of R^2 for a linearized Langmuir and Dubinin–Radushkevich isotherm were obtained. Overall, the results indicated no adequate agreement between the measured and predicted adsorption data by those linearized models, implying especially the lack of validity of the linearized Langmuir isotherm to model the adsorption of the heavy metals onto starch residues in aqueous solution. Both linear and non-linear fitting of the experimental data to the Freundlich model yield high R^2 in most cases with no great difference between linear and non-linear fitting. The results indicate that non-linear fitting of the measured data to the non-linear isotherm model could provide significantly more robust prediction compared to the linear fitting, which was due of the lack of total error achieved by non-linear adjustment, as reported by Zand and Abyaneh [38], during the evaluation of a wood-derived model in the removal of lead, manganese and copper. Overall, in this study, the results indicated that linearization of the Langmuir and Dubinin–Radushkevich isotherms to fit the experimental data may generate higher errors and significantly deviate the predicted adsorption capacity of a given adsorbent from the experimental data.

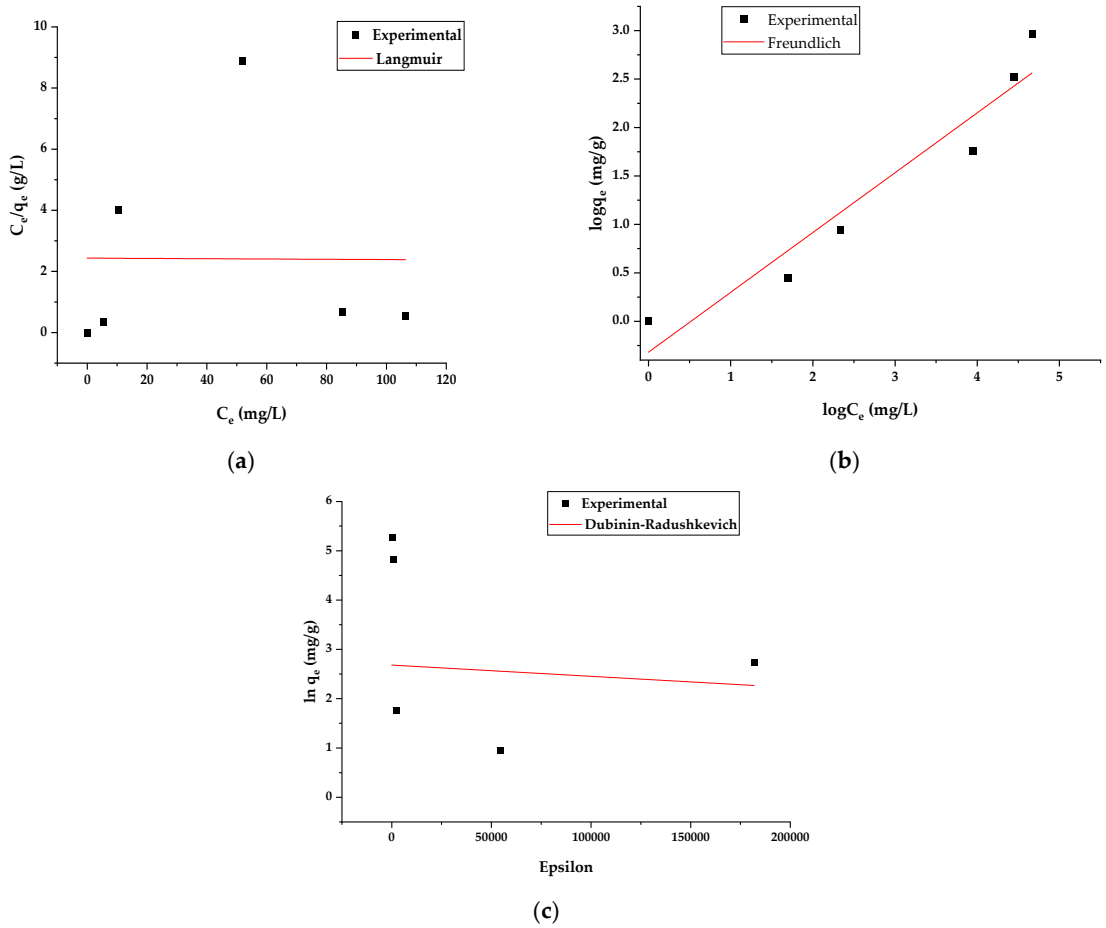

Figure 10. Linear modeling of the Cr (VI) adsorption isotherm using (**a**) Langmuir, (**b**) Freundlich and (**c**) Dubinin–Radushkevich model; at pH = 2, 55 °C and 0.14 g of adsorbent.

3.5. Thermodynamic Parameters

The values of ΔG° (kJ/mol), ΔS° (kJ $\times$ K^{-1}) and ΔH° (kJ/mol) were determined by applying van't Hoff's graphical method and Equations (12)–(14). The values of the thermodynamic parameters are given in Table 8.

Table 8. Thermodynamic parameters of Cr (VI) adsorption on residual plantain pulp at pH = 2, C_i = 200 mg/L and adsorbent dose = 0.5 g.

Temperature (K)	ΔH° (kJ/mol)	ΔS° (kJ $\times$ K^{-1})	ΔG° (kJ/mol)
306.9	85.25	−0.2	145.88
328.2	-	-	150.88
349.4	-	-	155.92

This positive value of ΔH° reveals that the process is endothermic for Cr (VI) elimination, so energy must be added to the system for the reaction to occur [39]; this behavior is consistent with the results in Table 4. The negative values of ΔS° indicate that the biomass–metal bonds are strong and that the active centers have a high selectivity and affinity with the metal, which means that the process has a low reversibility and implies that the adsorption of Cr (VI) on the residual plantain pulp is stable, which is common in processes that involve chemical adsorption and ion exchange [40]. The values reported for ΔG° at the different temperatures evaluated mean that at room temperature, the removal is favorable and spontaneous, and the conditions acquire as the temperature increases, as suggested by the increase in the module [41].

4. Conclusions

It was found that the best experimental conditions for adsorption using the bioadsorbents evaluated were at 55 °C, 0.14 g and 200 mg L^{-1}, and that the most influential variable in the process was the dose of adsorbent and temperature, reaching a maximum adsorption capacity of 64.46 mg/g. The characterization of the residual plantain pulp evidences the presence of hydroxyl, carbonyl and carboxyl groups, characteristic of lignin and cellulose and lignin, which are attributed to participation in the adsorption process. After the adsorption process, the decrease in the adsorption bands was observed, establishing that the process occurs by ion exchange when observing the change in the bands. The adsorption kinetics was adjusted to the pseudo-second order, Elovich and intraparticle diffusion models, while the isotherm was adjusted to the Freundlich and Dubinin–Radushkevich models, which suggests that the process is controlled by chemical reaction and occurs in multilayers and inside the pores of the adsorbent. Thermodynamic parameters determine that Cr (VI) adsorption is endothermic, with strong biomass–metal bonds that are favorable and spontaneous as temperature increases. The use of residual plantain pulp is suggested as a good alternative to adsorb Cr (VI) present in solution.

Author Contributions: Conceptualization, C.T.-T., A.V.-O. and Á.D.G.-D.; methodology, C.T.-T.; software, A.V.-O.; validation, C.T.-T., A.V.-O. and Á.D.G.-D.; formal analysis, C.T.-T., A.V.-O.; investigation, C.T.-T. resources, C.T.-T.; data curation, Á.D.G.-D.; writing—original draft preparation, Á.D.G.-D.; writing—review and editing, C.T.-T.; visualization, A.V.-O.; supervision, C.T.-T.; project administration, A.V.-O. and Á.D.G.-D.; funding acquisition, C.T.-T. All authors have read and agreed to the published version of the manuscript.

Funding: This research received no external funding.

Data Availability Statement: The data that support the findings of this study are available on request from the corresponding author, C.T.-T. upon reasonable request.

Acknowledgments: The authors thank to the Universidad de Cartagena to provide the materials, equipment, and laboratory facilities required to successfully conclude this research.

Conflicts of Interest: The authors declare no conflict of interest.

References

1. Cherdchoo, W.; Nithettham, S.; Charoenpanich, J. Removal of Cr(VI) from synthetic wastewater by adsorption onto coffee ground and mixed waste tea. *Chemosphere* **2019**, *221*, 758–767. [CrossRef] [PubMed]
2. Manjuladevi, M.; Anitha, R.; Manonmani, S. Kinetic study on adsorption of Cr(VI), Ni(II), Cd(II) and Pb(II) ions from aqueous solutions using activated carbon prepared from Cucumis melo peel. *Appl. Water Sci.* **2018**, *8*, 36. [CrossRef]
3. Parlayici, Ş.; Pehlivan, E. Comparative study of Cr(VI) removal by bio-waste adsorbents: Equilibrium, kinetics, and thermodynamic. *J. Anal. Sci. Technol.* **2019**, *10*, 15. [CrossRef]
4. Mullick, A.; Moulik, S.; Bhattacharjee, S. Removal of Hexavalent Chromium from Aqueous Solutions by Low-Cost Rice Husk-Based Activated Carbon: Kinetic and Thermodynamic Studies. *Indian Chem. Eng.* **2018**, *60*, 58–71. [CrossRef]
5. Chen, Y.; An, D.; Sun, S.; Gao, J.; Qian, L. Reduction and Removal of Chromium VI in Water by Powdered Activated Carbon. *Materials* **2018**, *11*, 269. [CrossRef]
6. Mondal, N.K.; Samanta, A.; Chakraborty, S.; Shaikh, W.A. Enhanced chromium(VI) removal using banana peel dust: Isotherms, kinetics and thermodynamics study. *Sustain. Water Resour. Manag.* **2017**, *4*, 489–497. [CrossRef]
7. Lee, C.-G.; Lee, S.; Park, J.-A.; Park, C.; Lee, S.J.; Kim, S.-B.; An, B.; Yun, S.-T.; Choi, J.-W. Removal of copper, nickel and chromium mixtures from metal plating wastewater by adsorption with modified carbon foam. *Chemosphere* **2017**, *166*, 203–211. [CrossRef]
8. Corral-Escárcega, M.C.; Ruiz-Gutiérrez, M.G.; Quintero-Ramos, A.; Meléndez-Pizarro, C.O.; Lardizabal-Gutiérrez, D.; Campos-Venegas, K. Use of biomass-derived from pecan nut husks (*Carya illinoinensis*) for chromium removal from aqueous solutions. column modeling and adsorption kinetics studies. *Rev. Mex. Ing. Qumica* **2017**, *16*, 939–953.
9. Gómez Aguilar, D.L.; Rodríguez Miranda, J.P.; Esteban Muñoz, J.A.; Betancur, J.F. Coffee Pulp: A Sustainable Alternative Removal of Cr (VI) in Wastewaters. *Processes* **2019**, *7*, 403. [CrossRef]
10. Tejada-Tovar, C.; Herrera-Barros, A.; Villabona-Ortíz, A. Assessment of Chemically Modified Lignocellulose Waste for the Adsorption of Cr (VI). *Rev. Fac. Ing.* **2020**, *29*, e10298. [CrossRef]
11. Vu, H.T.; Scarlett, C.J.; Vuong, Q.V. Phenolic compounds within banana peel and their potential uses: A review. *J. Funct. Foods* **2018**, *40*, 238–248. [CrossRef]
12. Ben-Ali, S.; Jaouali, I.; Souissi-Najar, S.; Ouederni, A. Characterization and adsorption capacity of raw pomegranate peel biosorbent for copper removal. *J. Clean. Prod.* **2017**, *142*, 244–271. [CrossRef]
13. Al-Jubory, F.K.; Mujtaba, I.M.; Abbas, A.S. Preparation and characterization of biodegradable crosslinked starch ester as adsorbent. *AIP Conf. Proc.* **2020**, *2213*, 020165. [CrossRef]
14. Villabona-Ortíz, A.; Tejada-Tovar, C.; Ruiz-Paternina, E.; Frías-González, J.D.; Blanco-García, G.D. Optimization of the Effect of Temperature and Bed Height on Cr (VI) Bioadsorption in Continuous System. *Rev. Fac. Ing.* **2020**, *29*, e10477. [CrossRef]
15. Ruiz-Paternina, E.B.; Villabona-Ortiz, Á.; Tejada-Tova, C.; Ortega-Toro, R. Estudio Termodinámico de la Remoción de Níquel y Cromo en Solución Acuosa usando Adsorbentes de Origen Agroindustrial. *Inf. Tecnol.* **2019**, *30*, 3–10. [CrossRef]
16. Maniglia, B.; Tapia-Blácido, D. Food Hydrocolloids Isolation and characterization of starch from babassu mesocarp. *Food Hydrocoll.* **2016**, *55*, 47–55. [CrossRef]
17. Villabona-Ortíz, A.; De Cartagena, U.; Tejada-Tovar, C.N.; Ortega-Toro, R. Modelling of the adsorption kinetics of Chromium (VI) using waste biomaterials. *Rev. Mex. Ing. Química* **2019**, *19*, 401–408. [CrossRef]
18. Tran, H.N.; You, S.-J.; Chao, H.-P. Thermodynamic parameters of cadmium adsorption onto orange peel calculated from various methods: A comparison study. *J. Environ. Chem. Eng.* **2016**, *4*, 2671–2682. [CrossRef]
19. Peng, S.-H.; Wang, R.; Yang, L.-Z.; He, L.; He, X.; Liu, X. Biosorption of copper, zinc, cadmium and chromium ions from aqueous solution by natural foxtail millet shell. *Ecotoxicol. Environ. Saf.* **2018**, *165*, 61–69. [CrossRef]
20. Tejada-Tovar, C.; Villabona-Ortíz, A.; Ruiz-Paternina, E.; Herrera-Barros, A.; Ortega-Toro, R. Characterization and use of agroindustrial by-products in the removal of metal ions in aqueous solution. *J. Teknol.* **2019**, *81*, 151–158. [CrossRef]
21. Schwantes, D.; Gonçalves, A.C.; Campagnolo, M.A.; Tarley, C.R.T.; Dragunski, D.C.; de Varennes, A.; dos Santos Silva, A.K.; Conradi, E. Chemical modifications on pinus bark for adsorption of toxic metals. *J. Environ. Chem. Eng.* **2018**, *6*, 1271–1278. [CrossRef]
22. Medellin-Castillo, N. Bioadsorción de plomo (II) presente en solución acuosa sobre residuos de fibras naturales procedentes de la industria ixtlera (Agave lechuguilla Torr. y Yucca carnerosana (TREL.) MCKELVEY). *Rev. Int. Contam. Ambient.* **2017**, *33*, 269–280. [CrossRef]
23. Rodriguez Narvaez, O.M.; Peralta-Hernandez, J.M.; Goonetilleke, A.; Bandala, E.R. Treatment technologies for emerging contaminants in water: A review. *Chem. Eng. J.* **2017**, *323*, 361–380. [CrossRef]
24. Mishra, A.; Tripathi, B.D.; Rai, A.K. Packed-bed column biosorption of chromium(VI) and nickel(II) onto Fenton modified Hydrilla verticillata dried biomass. *Ecotoxicol. Environ. Saf.* **2016**, *132*, 420–428. [CrossRef]
25. Chinyelu Ijeamaka, E.; Odebeatu Chinoso, C.; Obumselu Onyeka, F.; Iloamaeke Ifeoma, M.J.; Kammeje Tochukwu, J. Isotherm Studies of Adsorption of Cr (Vi) Ions onto Coconut Husk. *Int. J. Biochem. Biophys. Mol. Biol.* **2018**, *3*, 38. [CrossRef]
26. Mutongo, F.; Kuipa, O.; Kuipa, P.K. Removal of Cr(VI) from Aqueous Solutions Using Powder of Potato Peelings as a Low Cost Sorbent. *Bioinorg. Chem. Appl.* **2014**, *2014*, 1–7. [CrossRef]
27. Saranya, N.; Ajmani, A.; Sivasubramanian, V.; Selvaraju, N. *Hexavalent Chromium Removal from Simulated and Real Effluents Using Artocarpus Heterophyllus Peel Biosorbent—Batch and Continuous Studies, 265*; Elsevier B.V: Amsterdam, The Netherlands, 2018.

28. Kuppusamy, S.; Thavamani, P.; Megharaj, M.; Venkateswarlu, K.; Lee, Y.B.; Naidu, R. Oak (Quercus robur) Acorn Peel as a Low-Cost Adsorbent for Hexavalent Chromium Removal from Aquatic Ecosystems and Industrial Effluents. *Water Air Soil Pollut.* **2016**, *227*, 62. [CrossRef]
29. Ajmani, A.; Shahnaz, T.; Subbiah, S.; Narayanasamy, S. Hexavalent chromium adsorption on virgin, biochar, and chemically modified carbons prepared from Phanera vahlii fruit biomass: Equilibrium, kinetics, and thermodynamics approach. *Environ. Sci. Pollut. Res.* **2019**, *26*, 32137–32150. [CrossRef]
30. Azadi, F.; Saadat, S.; Karimi-Jashni, A. Experimental Investigation and Modeling of Nickel Removal from Wastewater Using Modified Rice Husk in Continuous Reactor by Response Surface Methodology. *Iran. J. Sci. Technol. Trans. Civ. Eng.* **2018**, *42*, 315–323. [CrossRef]
31. Nordin, N.; Asmadi, N.A.A.; Manikam, M.K.; Halim, A.A.; Hanafiah, M.M.; Hurairah, S.N. Removal of Hexavalent Chromium from Aqueous Solution by Adsorption on Palm Oil Fuel Ash (POFA). *J. Geosci. Environ. Prot.* **2020**, *08*, 112–127. [CrossRef]
32. Mahmood-Ul-Hassan, M.; Yasin, M.; Yousra, M.; Ahmad, R.; Sarwar, S. Kinetics, isotherms, and thermodynamic studies of lead, chromium, and cadmium bio-adsorption from aqueous solution onto Picea smithiana sawdust. *Environ. Sci. Pollut. Res.* **2018**, *25*, 12570–12578. [CrossRef]
33. Manirethan, V.; Gupta, N.; Balakrishnan, R.M.; Raval, K. Batch and continuous studies on the removal of heavy metals from aqueous solution using biosynthesised melanin-coated PVDF membranes. *Environ. Sci. Pollut. Res.* **2019**, *27*, 24723–24737. [CrossRef] [PubMed]
34. Ho, Y.S.; McKay, G. Pseudo-second order model for sorption processes. *Process Biochem.* **1999**, *34*, 451–465. [CrossRef]
35. Arim, A.L.; Neves, K.; Quina, M.; Gando-Ferreira, L.M. Experimental and mathematical modelling of Cr(III) sorption in fixed-bed column using modified pine bark. *J. Clean. Prod.* **2018**, *183*, 272–281. [CrossRef]
36. Rodrigues, E.; de Almeida, O.; Brasil, H.; Moraes, D.; Reis, M.A.L. Applied Clay Science Adsorption of chromium (VI) on hydrotalcite-hydroxyapatite material doped with carbon nanotubes: Equilibrium, kinetic and thermodynamic study. *Appl. Clay Sci.* **2019**, *172*, 57–64. [CrossRef]
37. Módenes, A.N.; de Oliveira, A.P.; Espinoza-Quiñones, F.R.; Trigueros, D.E.G.; Kroumov, A.; Bergamasco, R. Study of the involved sorption mechanisms of Cr(VI) and Cr(III) species onto dried Salvinia auriculata biomass. *Chemosphere* **2017**, *172*, 373–383. [CrossRef] [PubMed]
38. Zand, A.D.; Abyaneh, M.R. Adsorption of Lead, manganese, and copper onto biochar in landfill leachate: Implication of non-linear regression analysis. *Sustain. Environ. Res.* **2020**, *30*, 1–16. [CrossRef]
39. Labied, R.; Benturki, O.; Hamitouche, A.Y.E.; Donnot, A. Adsorption of hexavalent chromium by activated carbon obtained from a waste lignocellulosic material (*Ziziphus jujuba* cores): Kinetic, equilibrium, and thermodynamic study. *Adsorpt. Sci. Technol.* **2018**, *36*, 1066–1099. [CrossRef]
40. Romero-Cano, L.A.; García-Rosero, H.; Gonzalez-Gutierrez, L.V.; Baldenegro-Pérez, L.A.; Carrasco-Marín, F. Functionalized adsorbents prepared from fruit peels: Equilibrium, kinetic and thermodynamic studies for copper adsorption in aqueous solution. *J. Clean. Prod.* **2017**, *162*, 195–204. [CrossRef]
41. Haroon, H.; Ashfaq, T.; Gardazi, S.M.H.; Sherazi, T.A.; Ali, M.; Rashid, N.; Bilal, M. Equilibrium kinetic and thermodynamic studies of Cr(VI) adsorption onto a novel adsorbent of Eucalyptus camaldulensis waste: Batch and column reactors. *Korean J. Chem. Eng.* **2016**, *33*, 2898–2907. [CrossRef]